PHYSICAL REVIEW VOLUME 98, NUMBER 2 APRIL 15, 1955

Electric Quadrupole Interaction and Spin Echoes in Crystals

T. P. DAS AND A. K. SAHA
Institute of Nuclear Physics, Calcutta, India

(Received September 27, 1954; revised manuscript received November 30, 1954)

Bloom and Norberg and also Hahn and Herzog have observed spin echoes due to electric quadrupole interaction alone and also in the presence of a weak magnetic field in addition to electric quadrupole interaction, with Cl^{35} (spin $I=3/2$) nuclei in $NaClO_3$ crystal. They have explained these echoes theoretically for the particular case of $I=3/2$. We have calculated the spin-echo amplitudes to be expected under the above experimental conditions for nuclei of any general spin in crystals with axial symmetry. The opposite case of spin echoes in a strong magnetic field in the presence of weak electric quadrupole interaction is also discussed. The theoretical investigation leads to "slow beats" in this case also.

INTRODUCTION

IN the conventional spin-echo experiment,[1] we have a strong steady magnetic field, perpendicular to which a radio-frequency magnetic field is applied, and the free induction and echo signals following the application of the radio-frequency field in short pulses, is studied. However, in the case of many crystals, some of the nuclei have considerable electric quadrupole interaction with the surroundings. In such cases one can think of spin-echo experiments where the electric field gradient inside the crystal takes the place of the steady magnetic field. Such experiments have recently been carried out successfully by Hahn and Herzog[2] and also by Bloom and Norberg[3,4] in the case of chlorine nuclei in $NaClO_3$ crystal. They have also observed the modulation pattern obtained when a steady weak magnetic field is applied at an angle θ_0 to the axis of symmetry of the crystal. They have explained their observed results theoretically using a method similar to the one used earlier by Hahn and Maxwell.[5] We shall show in this paper how their results can be explained and extended to the case of nuclei with any general spin I, using the density matrix method of calculating spin-echo amplitudes developed by us in an earlier paper.[6] This paper is divided into three sections. In Sec. I, we take up the case of spin-echo signals for pure quadrupole coupling. In Sec. II, we examine the effect of a weak magnetic field superimposed on the electric quadrupole coupling, at an angle θ_0 to the axis of symmetry of the crystal. In Sec. III, the opposite case is treated, *viz.*, the one in which the electric quadrupole effect is small but the applied magnetic field is strong. As in our previous paper,[6] which we shall henceforth refer to as Paper I, we have not included the effects of the relaxation times T_1 and T_2, because from a phenomenological point of view, we expect their effects on the spin echoes in the present case to be the same as on the conventional spin echoes.[1] In a later paper we shall try to examine how the concept of density matrix[7] may be used in the context of the Bloembergen picture[8,9] of relaxation forces to introduce their effects directly into the spin-echo signal amplitudes.

SECTION I. PURE QUADRUPOLE CASE

As explained in Paper I, our method of calculating the spin-echo amplitudes essentially involves solution of the time-dependent Schrödinger equations for the spin system in the presence and absence of the rf pulses. If the Hamiltonian due to the electric quadrupole interaction be $\mathcal{H}_0$ and the additional perturbation due to the applied radio-frequency field be $\mathcal{H}'$, then if R and D represent the transformation matrices in the presence and absence of pulses respectively, then the Schrödinger equations in the two cases will be

$$i\hbar\frac{dR}{dt}=(\mathcal{H}_0+\mathcal{H}')R,\qquad i\hbar\frac{dD}{dt}=\mathcal{H}_0D. \tag{1}$$

We shall refer to R in the future as the "transition matrix" depicting the transformation in the state of the spin-system in the presence of a rf pulse and to D as the "free-precession matrix" depicting the transformation in the state of the spin-system in the absence of the rf pulses. If we now apply n rf pulses, then the net transformation matrix S, termed the "echo matrix," will be given by

$$S=D_nR_nD_{n-1}R_{n-1}\cdots D_2R_2D_1R_1, \tag{2}$$

the suffixes referring to the successive pulses. The density matrix[6] $\rho(t)$ for the spin system after the passage of the pulses will then be related to the initial density matrix before the pulses are applied by the

[1] E. L. Hahn, Phys. Rev. **80**, 580 (1950).
[2] E. L. Hahn and B. Herzog, Phys. Rev. **93**, 639 (1954).
[3] M. Bloom and R. Norberg, Phys. Rev. **93**, 638 (1954).
[4] M. Bloom, Phys. Rev. **94**, 1396 (1954).
[5] E. L. Hahn and D. E. Maxwell, Phys. Rev. **88**, 1070 (1952).
[6] Das, Saha, and Roy, Proc. Roy. Soc. (London) **A227**, 407 (1955).
[7] P. A. M. Dirac, *Quantum Mechanics* (Clarendon Press, Oxford, 1947), third edition, p. 132.
[8] Bloembergen, Purcell, and Pound, Phys. Rev. **73**, 679 (1948).
[9] R. K. Wangsness and F. Bloch, Phys. Rev. **89**, 728 (1953), have introduced T_1 and T_2 in the differential equations for the density matrix under certain restricted conditions and without using the detailed Bloembergen picture.

relation

$$\rho(t)=S\rho(0)S^{-1}. \tag{3}$$

In most experiments, where the rf coil producing the rf field is also the detector, we need the expectation value of I_x, the x component of the spin of the members of the spin system, after the passage of pulses. This is given by

$$\langle I_x\rangle=\mathrm{Tr}\{\rho(t)I_x\}=\mathrm{Tr}\{S\rho(0)S^{-1}I_x\}, \tag{4}$$

The Hamiltonian in the case of pure quadrupole coupling may be written down, in the irreducible tensor scalar product form[10,11] as

$$\mathcal{H}_0=\sum_r (Q)_r{}^2(\nabla\mathbf{E})_{-r}{}^2, \tag{5}$$

where the components $(Q)_r{}^2$ of the electric quadrupole moment tensor of the nucleus and $(\nabla\mathbf{E})_r{}^2$ of the field-gradient tensor are given by

$$\begin{aligned}(Q)_0{}^2&=\frac{eQ}{2I(2I-1)}(3I_0{}^2-\mathbf{I}^2),\\ (Q)_{\pm1}{}^2&=\mp(\tfrac{1}{2}\sqrt{6})\frac{eQ}{2I(2I-1)}\{I_\pm,I_0\},\\ (Q)_{\pm2}{}^2&=(\tfrac{1}{2}\sqrt{6})\frac{eQ}{2I(2I-1)}(I_\pm)^2,\end{aligned} \tag{6}$$

and

$$\begin{aligned}(\nabla\mathbf{E})_0{}^2&=\tfrac{1}{4}eq(3\cos^2\theta_0-1),\\ (\nabla\mathbf{E})_{\pm1}{}^2&=\pm(\tfrac{1}{4}\sqrt{6})eq\sin\theta_0\cos\theta_0\exp(\pm i\phi_0),\\ (\nabla\mathbf{E})_{\pm2}{}^2&=(\tfrac{1}{8}\sqrt{6})eq\sin^2\theta_0\exp(\pm2i\phi_0),\end{aligned} \tag{7}$$

with $I_0=I_z$ and $I_\pm=I_x\pm iI_y$; the notation $\{A,B\}$ refers to the anti-commutator $(AB+BA)$. Q is the scalar quadrupole moment defined by Casimir,[12] depending on the charge distribution within the nucleus. q is similarly the scalar quantity[10] defining the components of the field gradient tensor for axial symmetry depending on the charge distribution around the nucleus. ϕ_0 and θ_0 refer respectively to the azimuth and colatitude of the axis of the symmetry in the coordinate system chosen. If we now choose our coordinate system with the axis of symmetry as the z axis, we then have $\theta_0=0$, and we get,[13]

$$\mathcal{H}_0=P\hbar(3I_0{}^2-\mathbf{I}^2), \tag{8}$$

where

$$P=\frac{e^2Qq}{4\hbar I(2I-1)}. \tag{9}$$

Evidently the energy levels will be specified by the eigenvalues of I_z and the levels corresponding to eigenvalues $+m$ and $-m$ will coincide. We shall thus have in all, $(I+1)$ distinct energy levels for integral I and $(I+\frac{1}{2})$ for half-integral I. The spacing between the adjacent levels will be unequal, and we shall therefore have in all, I resonance frequencies for integral I, and $(I-\frac{1}{2})$ for half-integral, corresponding to the energy differences between successive levels [see Figs. 1 (A and C)]. The resonance frequency corresponding to the transitions $m\rightarrow(m-1)$ and $-m\rightarrow-(m-1)$ will thus be given by

$$\omega(m)=3P[m^2-(m-1)^2]=3P(2m-1). \tag{10}$$

Let the applied radio-frequency be that corresponding to the transitions,

$$\pm m_1\rightarrow\pm(m_1-1).$$

For brevity, we introduce the following notations:

$$\begin{aligned}E(m_1)&=aP\hbar,\\ E(m_1-1)&=bP\hbar,\\ a&=3m_1{}^2-I(I+1),\\ b&=3(m_1-1)^2-I(I+1),\end{aligned} \tag{11}$$

so that the resonance frequency in question is

$$\omega(m_1)=P(a-b). \tag{12}$$

If the radio-frequency magnetic field be applied at right angles to the symmetry axis, (i.e., the z-axis), then calling its direction that of x, the perturbing Hamiltonian will be

$$\mathcal{H}_1(t)=-\gamma\hbar I_x\cdot H_r\cos\omega(t-t_0), \tag{13}$$

where I_x is the x-component of the nuclear spin and $2H_r$ the amplitude of the radio-frequency field, ω being its frequency. Now, following the usual method[14] for dealing with time-dependent Hamiltonians, we have the matrix R given by,

$$\begin{aligned}R(t,t_0)&=\exp[-(i/\hbar)\mathcal{H}_0(t-t_0)]\cdot R^*(t,t_0),\\ R^*(t,t_0)&=\exp\left[-(i/\hbar)\int_{t_0}^{t}\mathcal{H}_1{}^*(t')dt'\right],\\ \mathcal{H}_1{}^*(t')&=\exp[(i/\hbar)\mathcal{H}_0(t'-t_0)]\cdot\mathcal{H}_1(t')\\ &\quad\times\exp[-(i/\hbar)\mathcal{H}_0(t-t_0)].\end{aligned} \tag{14}$$

In the present case, using (13),

$$\begin{aligned}\mathcal{H}_1{}^*(t')=&-\tfrac{1}{2}\omega_1\hbar\{\exp(3iP(t'-t_0)(2I_0-1))\\ &\cdot I_+[\exp(i\omega(t'-t_0))+\exp(-i\omega(t'-t_0))]\\ &+\exp(-3iP(t'-t_0)(2I_0+1))\cdot I_-[\exp(i\omega(t'-t_0))\\ &+\exp(-i\omega(t'-t_0))]\}.\end{aligned} \tag{15}$$

Using $\omega=\omega(m_1)$ and putting $t-t_0=t_w$, the rf pulse

[10] R. V. Pound, Phys. Rev. **79**, 685 (1950).

[11] Refer to M. K. Banerjee and A. K. Saha, Proc. Roy. Soc. (London) **A224**, 472 (1954). We have followed their notation closely.

[12] H. B. G. Casimir, Arch. du Musée Teyler, **8**, 202 (1936).

[13] R. Bersohn, J. Chem. Phys. **20**, 1505 (1952).

[14] P. A. M. Dirac, *Quantum Mechanics* (Clarendon Press, Oxford, 1947), third edition, p. 173.

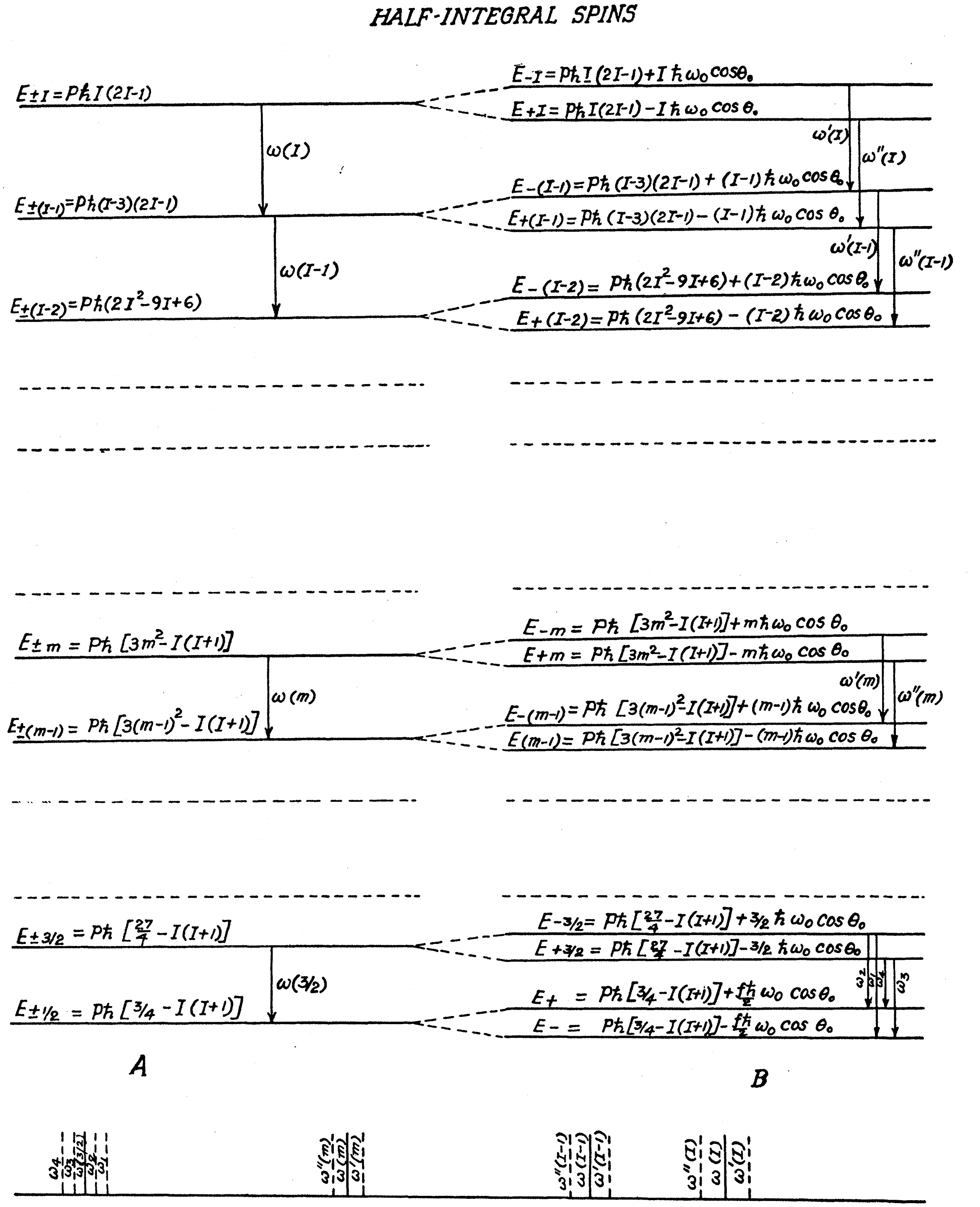

FIG. 1. A and B are energy-level diagrams for half-integral spins resulting from pure electric quadrupole interaction only, and also in the presence of a weak steady magnetic field. The solid lines in the lower part of the figure represent the pure quadrupole resonance frequencies and the dotted lines the resonance lines in the presence of the weak magnetic field.

width, the matrix elements of R may be easily found from (14) and (15). Thus we have

$$\langle m|R|m'\rangle=\exp\{-iPt_w[3m^2-I(I+1)]\}\delta_{mm'},\quad \text{for}\quad m\neq\pm m_1,\ \pm(m_1-1),$$

$$\begin{aligned}\langle\pm m_1|R|m'\rangle&=\cos(x\xi/2)\exp(-iPat_w)\delta_{m',\pm m_1}\\&\quad+i\sin(x\xi/2)\exp(-iPat_w)\delta_{m',\pm(m_1-1)},\\ \langle\pm(m_1-1)|R|m'\rangle&=\cos(x\xi/2)\exp(-iPbt_w)\delta_{m',\pm(m_1-1)}\\&\quad+i\sin(x\xi/2)\exp(-iPbt_w)\delta_{m',\pm m_1},\end{aligned}\tag{16}$$

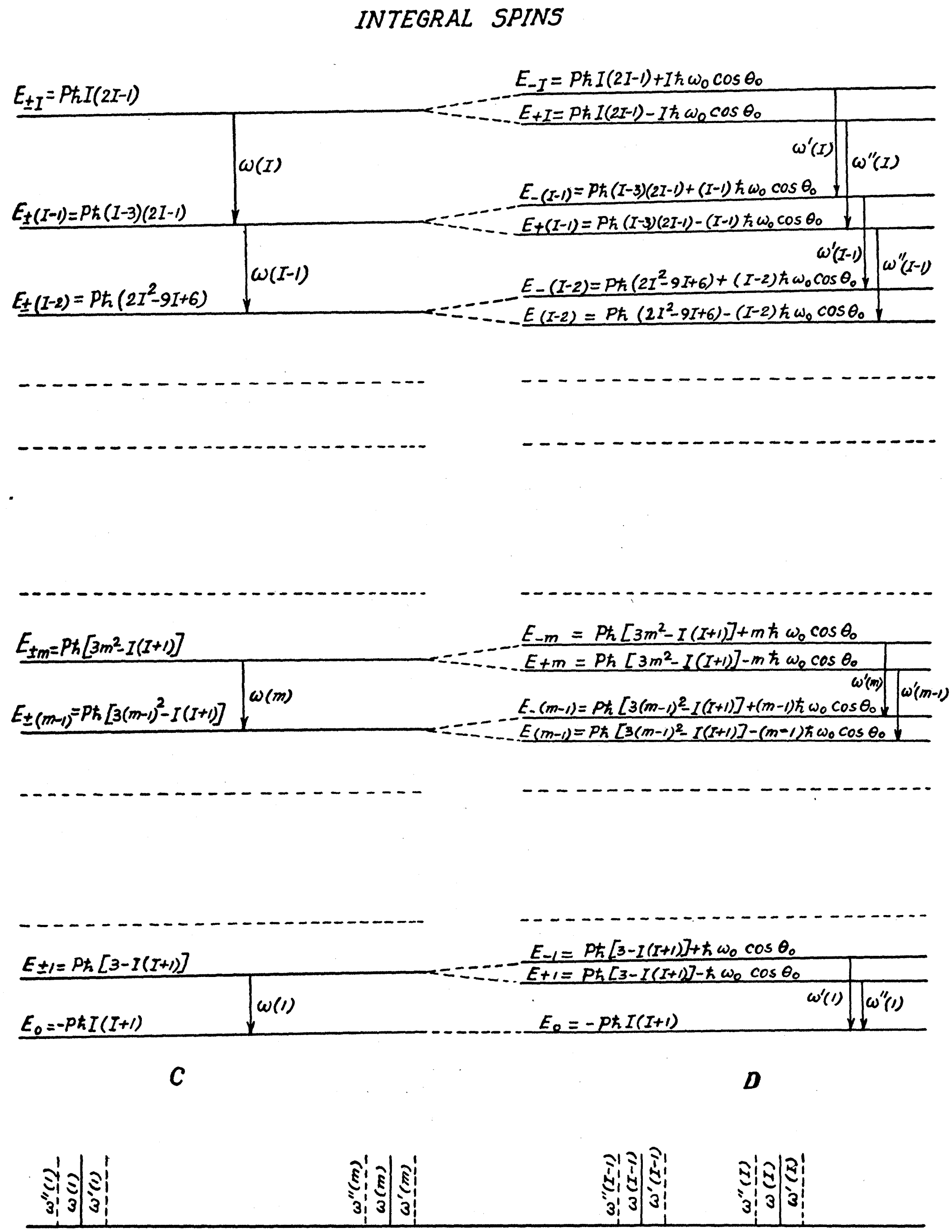

FIG. 1 (*continued*). C and D are energy-level diagrams for integral spins resulting from pure electric quadrupole interaction only, and also in the presence of a weak steady magnetic field. The solid lines in the lower part of the figure represent the pure quadrupole resonance frequencies and the dotted lines the resonance lines in the presence of the weak magnetic field.

where

$$x=[(I-m_1)(I+m_1+1)]^{\frac{1}{2}}. \tag{17}$$

In the absence of the rf field pulse, the free precession is given by the free precession matrix D, *viz.*,

$$D(t,t_0)=\exp[-(i/\hbar)\mathcal{H}_0(t-t_0)],$$

so that

$$\langle m|D(t,t_0)|m'\rangle =\exp\{-iP(t-t_0)[3m^2-I(I+1)]\}\delta_{mm'}, \tag{18}$$

for all m.

The density matrix at start, $\rho(0)$, is given by a normalized Boltzmann distribution,

$$\rho(0)=\frac{N}{2I+1}\exp\left[-\frac{P\hbar}{k\Theta}(3I_z^2-\mathbf{I}^2)\right], \tag{19}$$

where Θ is the absolute temperature and k the Boltzmann constant, N being the number of nuclei in the sample. If the spin-echo matrix at the end of a number of pulses be S, then we have the expectation value of I_x after these pulses given by (3). Remembering that $P\hbar/k\Theta\ll 1$, and S and I_x both commute with $\mathbf{I}^2$, we shall have

$$\langle I_x\rangle=\frac{N}{2I+1}\operatorname{Tr}\left(-\frac{3P\hbar}{k\Theta}SI_z^2S^{-1}I_x\right). \tag{20}$$

Using a pulse pattern of the type shown in Fig. 2 with pulse width t_w satisfying the usual conditions,[1] we have, following the procedure outlined in Paper I, the master matrices at the end of one and two pulses respectively given by the following equations.

Single pulse: $\tau<t<t_w$ (free induction signal)

$$\begin{aligned}\langle m|S_{\mathrm{I}}|m'\rangle&=\exp\{-iPt[3m^2-I(I+1)]\}\delta_{mm'},\\ &\qquad\text{for}\quad m\neq\pm m_1,\ \pm(m_1-1),\\ \langle\pm m_1|S_{\mathrm{I}}|m'\rangle&=a_1\delta_{m',\pm m_1}+c_1\delta_{m',\pm(m_1-1)},\\ \langle\pm(m_1-1)|S_{\mathrm{I}}|m'\rangle&=d_1\delta_{m',\pm m_1}+b_1\delta_{m',\pm(m_1-1)},\end{aligned} \tag{21}$$

with

$$\begin{aligned}a_1&=\exp(-iPat)\cdot\cos(x\xi/2),\\ b_1&=\exp(-iPbt)\cdot\cos(x\xi/2),\\ c_1&=i\exp(-iPat)\cdot\sin(x\xi/2),\\ d_1&=i\exp(-iPbt)\cdot\sin(x\xi/2).\end{aligned} \tag{22}$$

Two pulses: $t=(\kappa+\tau)$ (spin-echo signal)

$$\begin{aligned}\langle m|S_{\mathrm{II}}|m'\rangle&=\exp\{-iPt[3m^2-I(I+1)]\}\delta_{mm'},\\ &\qquad\text{for}\quad m\neq\pm m_1,\ \pm(m_1-1),\\ \langle\pm m_1|S_{\mathrm{II}}|m'\rangle&=a_2\delta_{m',\pm m_1}+c_2\delta_{m',\pm(m_1-1)},\\ \langle\pm(m_1-1)|S_{\mathrm{II}}|m'\rangle&=b_2\delta_{m',\pm m_1}+d_2\delta_{m',\pm(m_1-1)},\end{aligned} \tag{23}$$

where

$$\begin{aligned}a_2&=\cos^2(x\xi/2)\exp[-iPa(\kappa+\tau)]\\ &\qquad-\sin^2(x\xi/2)\exp[-iP(a\kappa+b\tau)],\\ b_2&=\tfrac{1}{2}i\sin(x\xi)\{\exp[-iPb(\kappa+\tau)]\\ &\qquad+\exp(-iP(b\kappa+a\tau)]\},\\ c_2&=\tfrac{1}{2}i\sin(x\xi)\{\exp[-iPa(\kappa+\tau)]\\ &\qquad+\exp(-iP(a\kappa+b\tau)]\},\\ d_2&=\cos^2(x\xi/2)\exp[-iPb(\kappa+\tau)]\\ &\qquad-\sin^2(x\xi/2)\exp[-iP(b\kappa+a\tau)].\end{aligned} \tag{24}$$

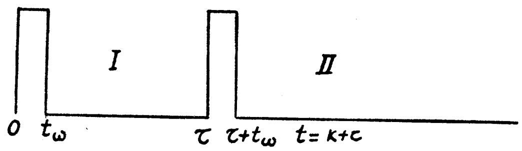

FIG. 2. Applied rf pulses.

Using Eqs. (21) and (23) together with (20), we get the expectation value of I_x after one and two pulses respectively as

$$\langle I_x\rangle=\frac{3NP\hbar}{(2I+1)k\Theta}x(2m_1-1)\sin(\omega(m_1)\cdot t), \qquad\text{(single pulse)} \tag{25}$$

$$\begin{aligned}\langle I_x\rangle=\frac{3NP\hbar}{(2I+1)k\Theta}&x(2m_1-1)\\ &\times\{\sin(x\xi)\cos^2(x\xi/2)\sin[\omega(m_1)\cdot t]\\ &-\sin(x\xi)\sin^2(x\xi/2)\sin[\omega(m_1)\cdot(t-2\tau)]\\ &+\sin(x\xi)\cos(x\xi)\sin[\omega(m_1)\cdot(t-\tau)]\},\end{aligned} \qquad\text{(two pulses).} \tag{26}$$

In case there is an inhomogeneity in q, and hence in P, there will be a corresponding inhomogeneity in $\omega(m_1)$. As in the case of echoes in a strong magnetic field, we can assume a Gaussian distribution in $\Delta\omega=\omega(m_1)-\omega$, with an rms value of $1/T_2^*$; we then get, on integrating the right-hand sides of (25) and (26) over $\Delta\omega$,

$$\begin{aligned}\langle I_x\rangle=\frac{3NP\hbar}{(2I+1)k\Theta}&x(2m_1-1)\sin(x\xi)\sin\omega t\\ &\times\exp(-t^2/2T_2^{*2}),\end{aligned} \qquad\text{(single pulse),} \tag{27}$$

$$\begin{aligned}\langle I_x\rangle=\frac{3NP\hbar}{(2I+1)k\Theta}&x(2m_1-1)\\ &\times\{\sin(x\xi)\cos^2(x\xi/2)\sin\omega t\cdot\exp(-t^2/2T_2^{*2})\\ &-\sin(x\xi)\sin^2(x\xi/2)\sin\omega(t-2\tau)\\ &\cdot\exp[-(t-2\tau)^2/2T_2^{*2}]+\sin(x\xi)\cos(x\xi)\\ &\times\sin\omega(t-\tau)\cdot\exp[-(t-\tau)^2/2T_2^{*2}]\},\end{aligned} \qquad\text{(two pulses).} \tag{18}$$

In Eq. (28), the first and third terms are easily identified with the free induction signals following the first and second pulses respectively while the second term gives an echo at $t=2\tau$. We have here assumed that the rf field is perpendicular to the symmetry axis in the crystal. But in the general case, the rf coil may make an angle θ_1 with the symmetry axis. In such a case, following the above procedure, first it may be shown that in the R-matrix we have now $\xi=\omega_1t_w\sin\theta_1$, and secondly the component of the magnetization contributing to the free induction or echo signals will now be proportional to $\langle I_x\rangle \sin\theta_1$. With these modifications the spin-echo amplitude will still be given by (28). These considerations bring our results in exact agreement with those of Bloom[3] and Norberg and Hahn[2] and Herzog, if we put $I=3/2$ and $m_1=3/2$. Thus for spin 3/2, the amplitude of the spin-echo signal is proportional to

$$(\sqrt{3}/2)\sin(\sqrt{3}\xi)\sin^2(\sqrt{3}\xi/2).$$

For a higher spin like 2 or 5/2, where we have two possible quadrupole resonance frequencies, the spin-echo amplitude to be expected for either frequency is easily found by putting down the corresponding values of m_1 and x in Eq. (28). In Table I, we have tabulated the values of the different resonance frequencies, and relative spin-echo amplitudes for spins 1, 3/2, 2, 5/2 due to pure quadrupole coupling alone.

TABLE I. Spin-echo amplitudes in pure quadrupole coupling case for $I=1$, 3/2, 2, 5/2.

Spin	Value of $P(I)$	Resonance frequencies	Spin-echo amplitudes
1	$\frac{e^2Qq}{\hbar}$	$3P(1)$	$\frac{NP(1)\hbar}{k\Theta}\sqrt{2}\sin(\sqrt{2}\xi)\sin^2(\xi/\sqrt{2})$
3/2	$\frac{e^2Qq}{12\hbar}$	$6P(3/2)$	$\frac{3NP(3/2)\hbar}{4k\Theta}2\sqrt{3}\sin(\sqrt{3}\xi)\sin^2\left(\frac{\sqrt{3}\xi}{2}\right)$
2	$\frac{e^2Qq}{24\hbar}$	$9P(2)$	$\frac{3NP(2)\hbar}{5k\Theta}6\sin(2\xi)\sin^2\xi$
		$3P(2)$	$\frac{3NP(2)\hbar}{5k\Theta}\sqrt{6}\sin(\sqrt{6}\xi)\sin^2\left(\frac{\sqrt{6}\xi}{2}\right)$
5/2	$\frac{e^2Qq}{40\hbar}$	$12P(5/2)$	$\frac{3NP(5/2)\hbar}{6k\Theta}4\sqrt{5}\sin(\sqrt{5}\xi)\sin^2\left(\frac{\sqrt{5}\xi}{2}\right)$
		$6P(5/2)$	$\frac{3NP(5/2)\hbar}{6k\Theta}2\sqrt{8}\sin(\sqrt{8}\xi)\sin^2(\sqrt{2}\xi)$

SECTION II. STRONG QUADRUPOLE COUPLING AND WEAK MAGNETIC FIELD

Suppose now we apply a weak steady magnetic field H_0 to the crystal at an angle θ_0 to the axis of symmetry; the Hamiltonian in the absence of the rf field will now be

$$\mathcal{H}=\mathcal{H}_0+\mathcal{H}', \tag{29}$$

where

$$\begin{aligned} H_0&=P\hbar(3I_0{}^2-\mathbf{I}^2),\\ \mathcal{H}'&=-\omega_0\hbar[I_0\cos\theta_0+\tfrac{1}{2}(I_++I_-)\sin\theta_0],\\ \omega_0&=\gamma H_0. \end{aligned} \tag{30}$$

It is now easy to see, using the perturbation theory for degenerate states, that the coincidence of the levels $+|m|$ and $-|m|$ discussed in Sec. I is destroyed and the energy levels are characterized by m, each m level being now quite distinct. For half-integral spins however, the two lowest levels are obtained by a mixing of the states corresponding to $m=\pm\frac{1}{2}$. The energy levels and eigenstates are tabulated in Figs. 1 (B and D) respectively for half-integral and integral spins.

We have

$$\begin{aligned} |+\rangle&=|\tfrac{1}{2}\rangle\cos\theta+|-\tfrac{1}{2}\rangle\sin\theta,\\ |-\rangle&=+|-\tfrac{1}{2}\rangle\cos\theta-|\tfrac{1}{2}\rangle\sin\theta,\\ \sin\theta&=-[(f+1)/2f]^{\frac{1}{2}},\quad \cos\theta=[(f-1)/2f]^{\frac{1}{2}}. \end{aligned} \tag{31}$$

For a half-integral spin $I=\frac{1}{2}(2p+1)$,

$$f=[1+(p+1)^2\tan^2\theta_0]^{\frac{1}{2}}. \tag{32}$$

We shall designate the new eigenstates by the numbers n, with the understanding that the n's correspond to the m's for all the levels of integral spins and for all the levels of half-integral spins, except $m=\pm\frac{1}{2}$. For this lowest pair of levels for half-integral spins, the n's correspond to $+$ and $-$.

Our discussion in this section will be divided into two parts. In the first part we shall take up the case of transitions between the lowest levels of half-integral spins and the next higher. In the second part we shall consider transition between levels other than the lowest for half-integral spins, and between all successive levels of integral spins, i.e., between levels where there is correspondence between the n's and m's.

(a) Transition between the Levels $\pm$ and the Next Higher Levels

The states next higher than the lowest levels will be those corresponding to $m=\pm 3/2$. It will be directly seen that the single frequency $\omega(3/2)=6P$ of the pure quadrupole case, is now replaced by four closely spaced frequencies given by

$$\omega_{1,2,3,4}=6P\pm\tfrac{1}{2}(3\pm f)\omega_0\cos\theta_0. \tag{33}$$

Let the applied radio-frequency be $\omega=6P$; to a first approximation we can then assume resonance conditions to exist for all these four frequencies. The R-matrix may be calculated as in Sec. I, with the following modifications. We have to replace $\mathcal{H}_0$ in Eq. (14) by $\mathcal{H}$ given by (29) and also we have to take matrix elements with the eigenstates of $\mathcal{H}$ as basis and not those of $\mathcal{H}_0$. A similar modification has to be applied to Eq. (18) to obtain the D-matrix in the present case. Also, exactly as in Sec. I, we can obtain in the present case the relevant matrix elements of S_{I} and S_{II}, the echo matrices after one and two pulses respectively. We can then use (20)[15] to find the expectation value of I_x after one and two pulses respectively to obtain the free-induction and echo amplitudes. We have the following equations for the expectation value of I_x after

[15] Properly we should use (4) with $\rho(0)$ defined by $\rho(0)=\exp(-\mathcal{H}/k\Theta)$, with $\mathcal{H}$ given by (29), but if we do not want to retain terms of the order of ω_0/P in the free-induction signal and echo amplitudes, we may just as well use (20) without much error.

one and two pulses, *viz.*,

$$\langle I_x\rangle=\frac{3NP\hbar}{k\Theta}\frac{2x}{2I+1}\sin(x\xi)\sin[\omega(\tfrac{3}{2})\cdot t]\cdot\left[\frac{f+1}{f}\cos\left(\frac{3-f}{2}(\omega_0\cos\theta_0)t\right)+\frac{f-1}{f}\cos\left(\frac{3+f}{2}(\omega_0\cos\theta_0)t\right)\right]\quad\text{(single pulse)},\quad(34)$$

$$\langle I_x\rangle=\frac{3NP\hbar}{k\Theta}\frac{2x}{2I+1}\sin(x\xi)\sin^2\left(\frac{x\xi}{2}\right)\sin[\omega(\tfrac{3}{2})\cdot(t-2\tau)]\times\left\{\left(\frac{f+1}{2f}\right)^2\cos\left(\frac{3-f}{2}(\omega_0\cos\theta_0)(t-2\tau)\right)+\left(\frac{f-1}{2f}\right)^2\cos\left(\frac{3+f}{2}(\omega_0\cos\theta_0)(t-2\tau)\right)+\frac{f^2-1}{2f^2}\left[\cos\left(\frac{3\omega_0\cos\theta_0}{2}(t-2\tau)\right)\cos\left(\frac{f\omega_0\cos\theta_0}{2}t\right)+\cos\left(\frac{3\omega_0\cos\theta_0}{2}t\right)\cos\left(\frac{f\omega_0\cos\theta_0}{2}(t-2\tau)\right)-\cos\left(\frac{3\omega_0\cos\theta_0}{2}t\right)\cos\left(\frac{f\omega_0\cos\theta_0}{2}t\right)\right]\right\}\quad\text{(two pulses)}.\quad(35)$$

In Eq. (35), only the terms giving rise to an echo at $t=2\tau$, *viz.*, the terms involving $\sin[\omega(3/2)\cdot(\kappa-\tau)]$ are given. In the presence of an inhomogeneity in q and a corresponding inhomogeneity in P, we have to integrate over a Gaussian distribution in $\Delta\omega=\omega(3/2)-\omega$ with rms value equal to $1/T_2{}^*$ as before. $\mathrm{Sin}(\omega(3/2)\cdot t)$ in (34) then gets replaced by $\sin\omega t\cdot\exp(-t^2/2T_2{}^{*2})$ and $\sin[\omega(3/2)\cdot(t-2\tau)]$ in (35) gets replaced by $\sin(\omega(t-2\tau))\cdot\exp[-(t-2\tau)^2/2T_2{}^{*2}]$, the latter exponential term showing the occurrence of the echo maximum at $t=2\tau$. It is evident that we get a modulation of the pure-quadrupole echo signal by the action of the weak z-field. If only a single spin-echo signal, corresponding to a pair of pulses with a fixed interval between them, be observed, then it will appear to have a modulation on account of all the terms in (35) involving ω_0. We term this modulation pattern "echo modulation." On the other hand, in echo envelope measurements with paired pulses of varying intervals τ only the last ω_0 terms, *viz.*, those multiplying the factor $(f^2-1)/2f^2$ will give rise to a modulation of the envelope, the other two terms being independent of τ at the instants of occurrence of the echoes, i.e., at $t=2\tau$. We term this modulation "envelope modulation." Besides this modulation of the echo envelope there will be the usual exponential damping due to the causes contributing to the transverse relaxation time. We shall not incorporate the effect of the latter here, but shall merely mention that as pointed out by Hahn and Maxwell,[5] to get a correct estimate of the present modulation effects from experimental echo envelopes, the latter have to be normalized first to correct for the above damping.

(b) The other important case that we have to consider is that in which the applied frequency corresponds to pure quadrupole frequencies $\omega(m_1)$ other than that between levels $\pm 3/2$ and $\pm 1/2$. In this case, each frequency $\omega(m_1)$ in the pure quadrupole case is broken up into a doublet $\omega(m_1)\pm\omega_0\cos\theta_0$ by the action of the weak magnetic field. Proceeding as in the previous two cases, we obtain the free induction and echo signals respectively as

$$\langle I_x\rangle=\frac{3NP\hbar}{k\Theta}\frac{x(2m_1-1)}{(2I+1)}\sin(x\xi)\sin\omega t\times\cos[\omega_0\cos\theta_0\cdot t]\exp\left(-\frac{t^2}{2T_2{}^{*2}}\right),$$

$$\langle I_x\rangle=\frac{3NP\hbar}{k\Theta}\frac{x(2m_1-1)}{(2I+1)}\sin(x\xi)\sin^2\left(\frac{x\xi}{2}\right)\sin[\omega(t-2\tau)]\times\cos[\omega_0\cos\theta_0(t-2\tau)]\times\exp[-(t-2\tau)^2/2T_2{}^{*2}].\quad(36)$$

This expression evidently holds for all the pure quadrupole resonance frequencies of a nucleus with integral spin I and for all those of half-integral spins except the lowest one, *viz.*, that between levels $\pm 3/2$ and $\pm 1/2$. It is evident from the expression (36), that in these cases we merely have an "echo modulation" and not any "envelope modulation."

SECTION III. STRONG STEADY MAGNETIC FIELD AND WEAK QUADRUPOLE COUPLING

In this case, the Hamiltonian in the absence of the rf field is given by

$$\mathcal{H}=\mathcal{H}_0+\mathcal{H}',$$

where

$$\mathcal{H}_0=-\gamma\hbar I_zH_z,\quad(37)$$

and

$$\mathcal{H}'=\frac{e^2qQ}{8I(2I-1)}\left[(3I_0{}^2-\mathbf{I}^2)(3\cos^2\theta_0-1)+\tfrac{3}{2}\sin\theta_0\cos\theta_0(e^{-i\phi_0}\{I_+,I_0\}+e^{i\phi_0}\{I_-,I_0\})+\tfrac{3}{4}\sin^2\theta_0(I_+{}^2e^{-2i\phi_0}+I_-{}^2e^{2i\phi_0})\right],\quad(38)$$

Q and q being defined as before, and θ_0 giving the angle between the symmetry axis and the z-direction, *viz.*, the direction of the steady field; $\{a,b\}$ represents the anticommutator $(ab+ba)$ as before. We then have the energy levels correct to the first order given by

$$E_m = -m\hbar\omega_z + \tfrac{1}{2}P\hbar(3\cos^2\theta_0 - 1)[3m^2 - I(I+1)], \quad (39)$$

the eigenstates being characterized by the magnetic quantum number m, and

$$P = \frac{e^2qQ}{4I(2I-1)\hbar}. \quad (9)$$

This case differs from the previous cases in that there is only one central frequency here, *viz.*, ω_z, about which we have a number of symmetrically placed components with frequency separations of the order of P. Hence all these frequencies will be more or less subjected to resonance simultaneously and so the R-matrix will no longer be of the simple type obtained in the preceding cases. There will now be matrix elements between all the levels and it thus becomes difficult to give a generalized treatment for spin I. We shall only give the results for a few important cases, *viz.*, $I=1$, 3/2, 2. The last one is important, because whereas in the first two cases there is only one symmetrical pair of lines, in this case there are two. The case of spins greater than $I=2$ may be worked out by following the general procedure outlined below.

The R-matrix may be found as usual by Eq. (14), employing the eigenvalues and eigenkets discussed above. We then find that if we agree to neglect terms of the order of P/ω in the amplitude of the spin-echo term, then the R-matrix is the same as the usual Rabi-Bloch matrix,[16] *viz.*,

$$\langle m|R|m'\rangle = \exp[it_w\{m\omega_z - P[3m^2 - I(I+1)] \times (3\cos^2\theta_0 - 1)/2\}]\cdot\langle m|R^*|m'\rangle,$$

with

$$\langle m|R^*|m'\rangle = \{(I+m)!(I-m)!(I+m')!(I-m')!\}^{\frac{1}{2}} \times \sin^{2I}(\xi/2)\, i^{(2I-m-m')} \times \sum_k \frac{(-)_k \cot^{(m+m'+2k)}(\xi/2)}{(m+m'+k)!(I-m-k)!(I-m'-k)!k!}, \quad (40)$$

where k takes up integral values restricted by the condition that none of the factorial terms in the denominator is to be negative.

The D-matrix will as usual be given by

$$D(t,t_0) = \exp[-(i/\hbar)\mathcal{H}(t-t_0)]. \quad (41)$$

The density matrix at start will be given by the Boltzmann distribution, *viz.*,

$$\rho(0) = \frac{N}{2I+1}\exp\left(-\frac{\mathcal{H}}{k\Theta}\right),$$

and if we are not interested in retaining terms of the order P/ω in the echo and free-induction signal amplitudes, we can safely take it as

$$\rho(0) = \frac{N}{2I+1}\exp\left(-\frac{\hbar\omega_z I_z}{k\Theta}\right). \quad (42)$$

We can now obtain the echo matrices S_{I} and S_{II} after one and two pulses respectively, using (40), (41) and (2). Using these matrices and Eq. (3), we get the density matrix after the passage of one and two pulses respectively. Using (4), we now obtain the following expressions for the free induction and echo signals[17] for spin $I=1$:

Free-induction signal:

$$\langle I_x\rangle = \frac{2N\hbar\omega_z}{(2I+1)k\Theta}\sin\xi\,\sin\omega_z t\,\cos(3Pt),$$

Spin-echo signal:

$$\langle I_x\rangle = \frac{2N\hbar\omega_z}{(2I+1)k\Theta}\sin\xi\,\sin^2(\xi/2)\,\sin[\omega_z(t-2\tau)] \times\{\cos\xi\,\cos(3Pt) - 2\cos^2(\xi/2)\cos[3P(t-2\tau)]\}, \quad (43)$$

where $\omega_z \pm 3P$ are the two frequencies into which the original resonance line due to the z-field alone is split up by the quadrupole interaction. We have to integrate these expressions over the inhomogeneity in the applied z-field as in Paper I; we then get the free-induction and spin-echo signals as

Free-induction signal:

$$\langle I_x\rangle = \frac{2}{3}\frac{N\hbar\omega}{k\Theta}\sin\xi\,\cos(3Pt)\cdot\exp\left(-\frac{t^2}{2T_2^{*2}}\right), \quad (44)$$

Spin-echo signal:

$$\langle I_x\rangle = \frac{2}{3}\frac{N\hbar\omega}{k\Theta}\sin\xi\,\sin^2(\xi/2) \cdot\{\cos\xi\,\cos 3Pt - 2\cos^2(\xi/2)\cos[3P(t-2\tau)]\}. \quad (45)$$

It is evident that in the echo-expression (45), only the first term in the brackets causes an "envelope-modulation." The resonance frequencies and the free induction and echo signal amplitudes for spins $I=1$, 3/2 and 2 have been tabulated in Table II. A check on the correctness of these echo amplitudes is obtained by putting $P=0$, when we get the expression $\frac{1}{3}I(I+1) \times (2I+1)\sin\xi\,\sin^2(\xi/2)$ for spin I, discussed in Paper I.

CONCLUSION

We have discussed above the two extreme cases of spin-echo formation in crystals with (a) strong quadru-

[16] F. Bloch and I. I. Rabi, Revs. Modern Phys. 17, 237 (1945).

[17] We have only given the results for the case when the symmetry axis of the axially symmetric electric field gradient tensor, at the sites of the resonant nuclei, coincides with the direction of the applied magnetic field, i.e., $\theta_0=0$.

TABLE II. Spin-echo amplitudes in the case of strong z-field and weak quadrupole coupling.

Spin	Value of $P(I)$	Resonance frequencies	Free-induction signal amplitude[a]	Echo signal amplitude[a]
1	$\frac{e^2Qq}{4\hbar}$	$\omega_z \pm 3P(1)$	$\frac{2}{3}\frac{N\hbar\omega}{k\Theta}S\cos(3P(1)t)$	$\frac{4}{3}\frac{N\hbar\omega}{k\Theta}S^3C\{(C^2-S^2)\cos(3Pt)-2C^2\cos[3P(t-2\tau)]\}$
3/2	$\frac{e^2Qq}{12\hbar}$	$\omega_z \pm 6P(3/2)$	$\frac{N\hbar\omega}{k\Theta}SC[1+\frac{3}{2}\cos(6P(3/2)t)]$	$\frac{1}{2}\frac{N\hbar\omega}{k\Theta}S^3C\{-2(2C^2-S^2)^2+6C^2(C^2-2S^2)\cos(6P\tau)$ $-9C^4\cos[6P(t-2\tau)]+3S^2(2C^2-S^2)\cos(6Pt)$ $+6C^2(C^2-2S^2)\cos[6P(t-\tau)]\}$
2	$\frac{e^2Qq}{24\hbar}$	$\omega_2 \pm 9P(2)$ $\omega_z \pm 3P(2)$	$\frac{4N\hbar\omega}{5k\Theta}SC[2\cos 9Pt+3\cos 3Pt]$	$\frac{2}{5}\frac{N\hbar\omega}{k\Theta}S^3C\{-16C^6\cos 9P(t-2\tau)$ $-4S^4(S^2-29C^4+86C^6S^2+20C^6)\cos(9Pt)$ $+12C^6(C^2-3S^2)(C^4+S^4)\cos[3P(3t-4\tau)]$ $+24C^4S^2[2S^2(S^2-C^2)+C^4(2+C^2)]\cos[3P(3t-2\tau)]$ $+12C^4[C^6-C^4S^2-11S^4C^2+17S^6-24S^8]\cos 3P(t-4\tau)$ $-36C^2(C^8-2S^4C^4+6S^6C^2-5S^8+4S^{10})\cos 3P(t-2\tau)$ $+12(-S^6+7S^4C^2-13S^2C^4+3C^2)\cos(3Pt)$ $+24S^2C^2(C^6-C^4S^2+C^2S^4-3S^6+2S^8)\cos[3P(t+2\tau)]\}$

[a] C and S denote $\cos(\xi/2)$ and $\sin(\xi/2)$ respectively. In some places, due to lack of space the brackets denoting the spin to which P refers have been omitted. In these cases, the P's naturally stand for the $P(I)$'s of the corresponding rows.

pole interaction and weak magnetic field and (b) weak quadrupole interaction and strong magnetic field. Experiments in the former case have already been reported. But there are as yet no experimental results in the latter case. In some cases, such as in Al^{27} resonance in Al_2O_3 crystal, as Pound[9] points out, the second order perturbation due to electric quadrupole interaction is fairly appreciable. In such cases we expect some departure from the results obtained by the method detailed above. Nevertheless, using a second order perturbation treatment to handle the electric quadrupole interaction, we can obtain the spin-echo amplitudes in these cases, using the rudiments of our method. Besides, we have only discussed the situation when the strong magnetic field and the symmetry axis of the crystal coincide. We shall subsequently publish the results of calculation for the case in which the symmetry axis of the crystal makes an angle θ_0 with the strong magnetic field. Of course, the most general case would be one of "intermediate coupling," where the quadrupole interaction and the interaction with the z-field are of the same order. In this case, as Feld and Lamb[18] have discussed, we have to solve a secular equation to obtain the energy levels and eigenkets of the total Hamiltonian (29), the two terms $\mathcal{H}_0$ and $\mathcal{H}'$ being now of the same order. A complete solution of this secular equation (usually cubic, for spin 1 and higher than cubic for spins $I>1$) can only be obtained numerically. Using the energy values and eigenstates so obtained we can then find the R and D matrices using Eqs. (14) and (18). Then, proceeding as in the previous cases, the free-induction and echo amplitudes may be found by evaluating $\langle I_x \rangle$ after one and two pulses respectively.

The authors are indebted to Professor M. N. Saha for his keen interest in the progress of the work. They are also grateful to Mr. D. K. Roy and Mr. M. K. Banerjee for some helpful discussions.

[18] B. T. Feld and W. E. Lamb, Phys. Rev. 67, 15 (1945).